

A Dual-Functional Zn-MOF Probe for Detecting Fe^{3+} and $Cr_2O_7^{2-}$

Xue Wang¹, Xiao Li¹, Zhongmin Su^{1,2*}

¹*School of Chemical and Environmental Engineering, Jilin Provincial Science and Technology Innovation Centre of Optical Materials and Chemistry, Jilin Provincial International Joint Research Center of Photo-functional Materials and Chemistry, Changchun University of Science and Technology, Changchun, China*

²*State Key Laboratory of Supramolecular Structure and Materials, Institute of Theoretical Chemistry, College of Chemistry, Jilin University, Changchun, China*

*Corresponding Author. Email: zmsu@cust.edu.cn

Abstract. A zinc-containing metal-organic framework, formulated as $[Zn\text{ (IPA)}(\text{tatrz})_{0.5}(\text{H}_2\text{O})]$, was successfully constructed via a mixed-ligand strategy employing isophthalic acid (H₂IPA) and an anthracene-functionalized triazole ligand (tatrz). Solid-state fluorescence spectroscopy reveals a distinct emission peak at 525 nm for the synthesized Zn-MOF. Leveraging this pronounced luminescence, the material was engineered as a highly efficient dual-responsive fluorescent sensor capable of selective and sensitive detection toward Fe^{3+} and $Cr_2O_7^{2-}$ ions. The sensor demonstrates high sensitivity and a low detection limit, and its excellent selectivity in complex matrices was confirmed through systematic anti-interference experiments. Mechanistic investigation indicates that the fluorescence quenching response originates primarily from an inner filter effect. In summary, the Zn-MOF material shows promising potential as a high-performance fluorescence sensing platform for monitoring environmental pollutants.

Keywords: zinc metal-organic framework, fluorescence sensing, dual-function

1. Introduction

Metal-organic framework materials demonstrate significant potential for a wide range of applications due to their versatile functionalities [1,2]. Their tunable pore structures and diverse active sites provide unique advantages for the development of fluorescent sensors. Among them, Zn-based MOFs have attracted attention owing to the d¹⁰ electron configuration of Zn²⁺ ions, which helps avoid ligand field quenching and typically offers excellent photostability [3]. The development of fluorescent sensors capable of selective and sensitive detection of specific ions holds important scientific value for fields such as environmental monitoring and biological analysis. For example, Fe^{3+} ions play a critical role in biological systems, and their concentration imbalance may disrupt cellular metabolism and lead to related health issues [4]. $Cr_2O_7^{2-}$ is a typical industrial pollutant that poses long-term threats to ecological safety and public health [5]. Therefore, the development of fluorescent sensing materials capable of efficiently and simultaneously detecting Fe^{3+} and $Cr_2O_7^{2-}$

has emerged as a significant research direction in this field. In this work, a Zn-based MOF was synthesized by a solvothermal method employing isophthalic acid and an anthracene-functionalized triazole ligand. The Zn-MOF maintains crystalline integrity and fluorescence performance in aqueous media and across a defined temperature window, as confirmed by comprehensive stability studies. Sensing evaluations revealed pronounced fluorescence quenching toward both Fe^{3+} and $\text{Cr}_2\text{O}_7^{2-}$. The quenching mechanism, investigated via UV-Vis absorption and fluorescence lifetime analyses, is attributed predominantly to an inner filter effect.

2. Experimental

2.1. Materials and characterization

All analytical-grade reagents were used as received without further purification. The tatrz ligand was synthesized according to a previously reported method [6]. Single-crystal X-ray diffraction data for the Zn-MOF were collected at 298 K on a Bruker D8 VENTURE diffractometer equipped with a graphite monochromator and Mo K α radiation ($\lambda = 0.71073 \text{ \AA}$). The structure was solved and refined with the SHELXL-97 program using full-matrix least-squares techniques.

2.2. Preparation of Zn-MOF $[\text{Zn}(\text{IPA})(\text{tatrz})_{0.5}(\text{H}_2\text{O})]$

$\text{Zn}(\text{NO}_3)_2 \cdot 6\text{H}_2\text{O}$ (30 mg, 0.10 mmol), H_2IPA (12.5 mg, 0.075 mmol), and tatrz (9 mg, 0.03 mmol) were added to a solvent mixture of DMF and H_2O (4 mL:4 mL). After stirring at 25°C for 20 min, the mixture was transferred to a 25 mL Teflon-lined autoclave. The autoclave was heated at 100 °C for 3 d and then cooled naturally to 25 °C, yellow block crystals were obtained. Filtration of the reaction mixture, followed by washing with DMF and air drying, afforded the target compound (81% yield).

3. Results and discussion

3.1. Structural description and discussion of Zn-MOF

Single-crystal X-ray diffraction unveils that Zn-MOF (CCDC: 2385902) features a triclinic lattice in space group P-1 (Table 1). A Zn^{2+} , half a tatrz, an isophthalic acid, and a water molecule are located in the asymmetric unit (Figure 1a). The Zn^{2+} resides in a distorted square-pyramidal coordination environment. To complete the five-coordinate environment, the Zn (II) center binds to three oxygen donors from two μ_2 -bridging isophthalic acid linkers, one nitrogen donor from a tatrz ligand, and one water molecule. Here, each isophthalic acid linker serves in a $\mu_2\text{-}\eta^3\text{: }\eta^3$ bridging mode. (Figure 1b). The zinc centers are initially linked by isophthalic acid to form one-dimensional Zn-O chains; these chains are then cross-linked through tatrz ligands, extending into a one-dimensional framework (Figure 1c). As shown in Figure 1d, the one-dimensional chains further stack in an ordered fashion, giving rise to a three-dimensional architecture.

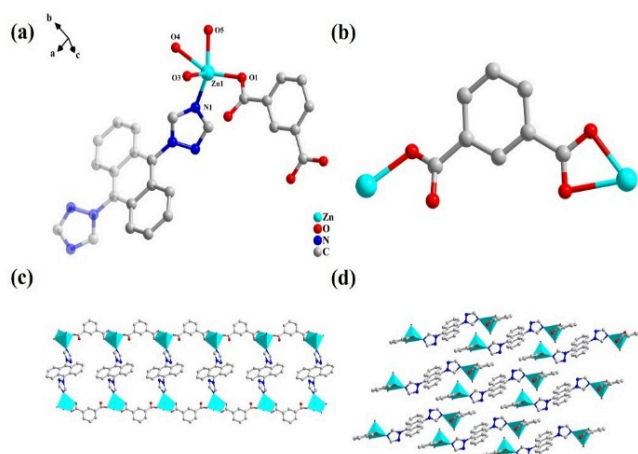


Figure 1. (a) The asymmetric unit. (b) The coordination mode of isophthalic acid ligands. (c) 1D structure diagram. (d) 3D structure diagram

Table 1. Key crystallographic parameters and refinement statistics for Zn-MOF

| Parameter | Value / Description |
|---------------------------------------|---|
| Chemical formula | $C_{17}H_{12}N_3O_5Zn$ |
| Molecular mass | 403.67 g/mol |
| Crystal system | Triclinic (space group P-1) |
| Unit cell (\AA , $^\circ$) | $a=8.3915(6)$, $b=10.0252(8)$, $c=12.0142(9)$; $\alpha=103.317(3)$, $\beta=107.409(3)$, $\gamma=109.107(3)$ |
| Volume (\AA^3) | 848.74(11) |
| Data collection | MoK α radiation ($\lambda=0.71073 \text{ \AA}$), $2\theta=4.8-50.138^\circ$, indices h (-9,9), k (-11,11), l (-14,14) |
| R factors ($I \geq 2\sigma$) | $R_1=0.1349$, $wR_2=0.3215$ |
| R factors (all) | $R_1=0.1438$, $wR_2=0.3362$ |

Measurement temperature: 273.15 K; calculated density: 1.58 g/cm³; $\mu=1.481 \text{ mm}^{-1}$; crystal size: 0.15×0.1×0.1 mm³; independent reflections: 2874 (Rint=0.0578); goodness-of-fit: 1.592.

3.2. Material characterization

The FTIR spectrum of Zn-MOF is shown in Figure 2a. The stability of Zn-MOF was subsequently investigated. The PXRD patterns of samples immersed in water for different durations (Figure 2b) match well with the simulated pattern, indicating excellent water stability. TGA analysis (Figure 2c) reveals a mass loss of 4.90% below 170 °C, attributed to the removal of water molecules, which is consistent with the theoretical water content (4.60%). This result demonstrates the good thermal stability of Zn-MOF. Furthermore, the solid-state fluorescence spectrum of Zn-MOF (Figure 2d) exhibits a strong emission peak at 525 nm. Compared with the free ligand (emission at 528 nm), a blue shift of about 3 nm is observed, mainly resulting from the coordination between Zn²⁺ and the ligand, which suppresses intramolecular rotation and vibration, thereby reducing non-radiative decay. Meanwhile, this coordination also modulates the π conjugation and chargetransfer properties of the anthracene moiety. Although isophthalic acid does not directly participate in the luminescence

process, it helps to extend the framework and stabilize the coordination geometry, further enhancing the structural rigidity and ultimately improving the luminescence efficiency.

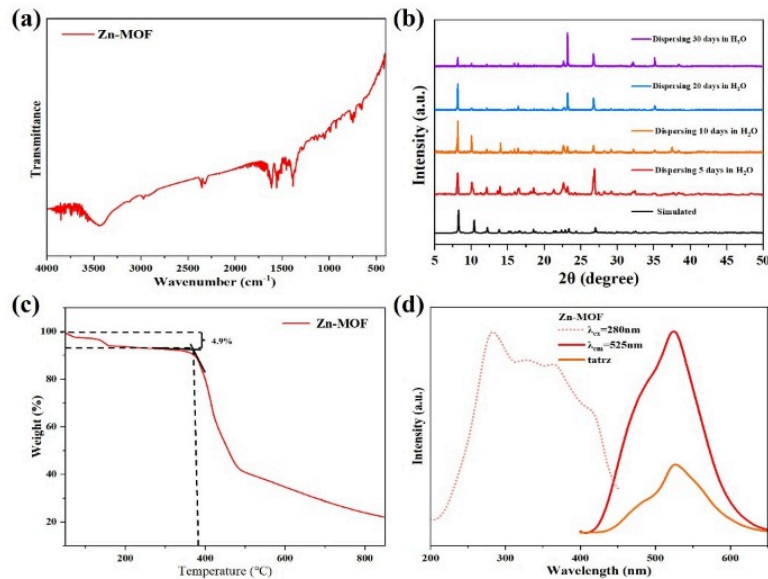


Figure 2. (a) FTIR spectra. (b) PXRD after soaking in water for different times. (c) TG curves. (d) The solid-state Excitation and Emission spectra

3.3. Ion sensing

The fluorescence sensing performance of Zn-MOF was systematically evaluated by investigating its fluorescence response toward a series of metal cations and anions. Among the metal ions tested, including Ag^+ , K^+ , Cd^{2+} , Mg^{2+} , Ni^{2+} , Pb^{2+} , Cu^{2+} , Co^{2+} , Ca^{2+} , Zn^{2+} , Al^{3+} , Cr^{3+} , Bi^{3+} , and Fe^{3+} , only Fe^{3+} induced a pronounced fluorescence quenching effect, which exhibited a clear positive correlation with Fe^{3+} concentration (Figure 3a, 3b). The Stern-Volmer plot displayed excellent linearity in the low-concentration region (Figure 3c), and the calculated detection limit for Fe^{3+} was determined to be $2.15\text{ }\mu\text{M}$. Anti-interference experiments further confirmed the high selectivity of the material, as a significant decrease in fluorescence intensity was observed only in the presence of Fe^{3+} (Figure 4a).

In the assessment of anion sensing performance, tests conducted on a range of anions, OH^- , Cl^- , CO_3^{2-} , HCO_3^- , Br^- , CH_3COO^- , BrO_3^- , F^- , and $\text{Cr}_2\text{O}_7^{2-}$ showed that Zn-MOF exhibited specific fluorescence quenching only toward $\text{Cr}_2\text{O}_7^{2-}$. This quenching effect increased progressively with increasing $\text{Cr}_2\text{O}_7^{2-}$ concentration (Figure 3d, 3e). The Stern-Volmer plot exhibits good linearity in the low-concentration region (Figure 3f), yielding a detection limit of $1.56\text{ }\mu\text{M}$ for $\text{Cr}_2\text{O}_7^{2-}$. Selectivity tests further confirm the specific recognition toward $\text{Cr}_2\text{O}_7^{2-}$, with distinct fluorescence changes observed only in its presence (Figure 4b). In summary, the developed Zn-MOF-based sensor demonstrates outstanding analytical performance for Fe^{3+} and $\text{Cr}_2\text{O}_7^{2-}$ detection, characterized by high sensitivity, excellent selectivity, and reliable concentration-dependent response.

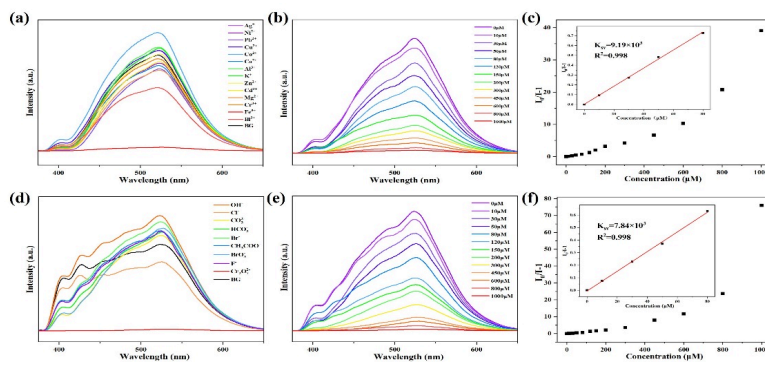


Figure 3. (a) Fluorescence spectra after addition of metal ions. (b) Fluorescence spectra in the presence of Fe^{3+} concentrations. (c) S-V plot with increasing Fe^{3+} concentration. (d) Fluorescence spectra after addition of anions. (e) Fluorescence spectra in the presence of $\text{Cr}_2\text{O}_7^{2-}$ concentration. (f) S-V plot with increasing $\text{Cr}_2\text{O}_7^{2-}$ concentration

3.4. Fluorescence sensing mechanism

To clarify the quenching mechanism, the interactions of Zn-MOF with Fe^{3+} and $\text{Cr}_2\text{O}_7^{2-}$ were examined. The PXRD patterns after ion exposure closely align with the simulated one (Figure 4c), confirming that the framework remains intact and that structural collapse does not drive the quenching. Comparative UV-Vis absorption and fluorescence spectra reveal partial spectral overlap between the analytes and Zn-MOF (Figure 4d, 4e), suggesting that quenching could proceed via either inner filter effect (IFE) or fluorescence resonance energy transfer (FRET). However, the nearly unchanged fluorescence lifetime upon ion addition (Figure 4f) indicates that IFE is the dominant pathway, ruling out significant FRET contribution.

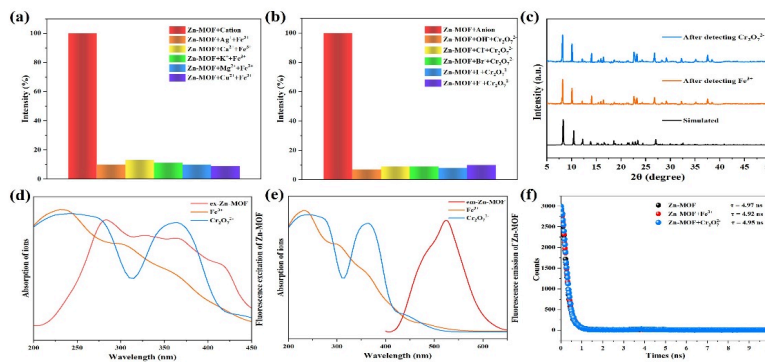


Figure 4. (a) Anti-interference test for sensing $\text{Cr}_2\text{O}_7^{2-}$. (b) Anti-interference test for sensing Fe^{3+} . (c) PXRD patterns after detecting Fe^{3+} and $\text{Cr}_2\text{O}_7^{2-}$. (d) Excitation-absorption spectral coincidence of crystal with Fe^{3+} and $\text{Cr}_2\text{O}_7^{2-}$. (e) Emission-absorption spectral coincidence of crystal with Fe^{3+} and $\text{Cr}_2\text{O}_7^{2-}$. (f) Evolution of the luminescence decay curves of the MOF in response to the addition of Fe^{3+} and $\text{Cr}_2\text{O}_7^{2-}$

4. Conclusion

In summary, this study successfully synthesized and characterized a structurally stable Zn-MOF with excellent fluorescence properties. This material serves as an efficient dual-functional fluorescent sensor for the response of Fe^{3+} and $\text{Cr}_2\text{O}_7^{2-}$, demonstrating high sensitivity and strong anti-interference capability. Mechanistic investigations indicate that the fluorescence quenching is

mainly due to an inner filter effect. These findings highlight the value of the Zn-MOF in the field of environmental monitoring via fluorescence sensing.

References

- [1] Bao, G.-M.; Wei, X.; Li, W.; Dou, Z.-C.; Cai, Z.-Q.; Xia, Y.-F.; Sandra, A.; Huang, J.-P.; Yuan, H.-Q.(2025) Instrument-free detection of natamycin in beer and wastewater based on Eu-MOF ratiometric fluorescence response. *Sensors and Actuators B: Chemical*, 422, 136696.
- [2] Chu, F.; Wei, X.; Lu, B.; Zhao, G.; Li, Y.; Yang, K.; Zhu, Z.; Su, T.; Lü, H.(2024) Flexible encapsulation polyoxometalate with electrostatically interaction into metal-organic framework for ultra-deep aerobic oxidation desulfurization of diesel via a biomimetic approach in deep eutectic solvents. *Chemical Engineering Journal*, 481.
- [3] Song, X.; Zhao, Q.; Hou, X.; Liu, S.; Luo, L.; Ren, Y.(2025) Three luminescent Zn/Cd-based MOFs for detecting antibiotics/nitroaromatic compounds and quenching mechanisms study. *Journal of Molecular Structure*, 1324, 140813.
- [4] Zhang, S.-R.; Zhang, W.-T.; Li, X.; Xu, G.-J.; Xie, W.; Xu, Y.-H.; Xu, N.; Su, Z.-M.(2025) Multifunctional Lanthanide Metal–Organic Frameworks Act as Fluorescent Probes for the Detection of $\text{Cr}_2\text{O}_7^{2-}$, Fe^{3+} , and TNP, White Light-Emitting Diodes, and Luminescence Thermometers. *Inorganic Chemistry*, 64 (6), 2990-2999.
- [5] Fan, L.; Zhang, J.; Zhao, Y.; Sun, C.; Li, W.; Chang, Z.(2024) A robust Eu-MOF as a multi-functional fluorescence sensor for detection of benzaldehyde, Hg^{2+} , and $\text{Cr}_2\text{O}_7^{2-}/\text{CrO}_4^{2-}$. *Microchemical Journal*, 196, 109712.
- [6] Liu, J.-Y.; Wang, Q.; Zhang, L.-J.; Yuan, B.; Xu, Y.-Y.; Zhang, X.; Zhao, C.-Y.; Wang, D.; Yuan, Y.; Wang, Y.; et al. (2014) Anion-Exchange and Anthracene-Encapsulation within Copper(II) and Manganese(II)-Triazole Metal-Organic Confined Space in a Single Crystal-to-Single Crystal Transformation Fashion. *Inorganic Chemistry*, 53 (12), 5972-5985.